

Multi-mode RWM Analysis of NSTX High Beta Plasmas



J.M. Bialek¹, S.A. Sabbagh¹, A. Boozer¹,
L. Delgado-Aparicio², S.P. Gerhardt²

¹Department of Applied Physics, Columbia University, NY, NY

²Plasma Physics Laboratory, Princeton University, Princeton, NJ

2010 NSTX Results & Theory Review

December 1, 2010

Princeton, N.J. - PPPL

College W&M
Colorado Sch Mines
Columbia U
Comp-X
General Atomics
INEL
Johns Hopkins U
LANL
LLNL
Lodestar
MIT
Nova Photonics
New York U
Old Dominion U
ORNL
PPPL
PSI
Princeton U
Purdue U
Sandia NL
Think Tank, Inc.
UC Davis
UC Irvine
UCLA
UCSD
U Colorado
U Maryland
U Rochester
U Washington
U Wisconsin

V1.0

Culham Sci Ctr
U St. Andrews
York U
Chubu U
Fukui U
Hiroshima U
Hyogo U
Kyoto U
Kyushu U
Kyushu Tokai U
NIFS
Niigata U
U Tokyo
JAEA
Hebrew U
Ioffe Inst
RRC Kurchatov Inst
TRINITI
KBSI
KAIST
POSTECH
ASIPP
ENEA, Frascati
CEA, Cadarache
IPP, Jülich
IPP, Garching
ASCR, Czech Rep
U Quebec

VALEN model of NSTX includes conducting structure, coils, and sensors

- High beta, low aspect ratio

- $R = 0.86$ m, $A > 1.27$

- $I_p < 1.5$ MA, $B_t = 5.5$ kG

- $\beta_t < 40\%$, $\beta_N < 7.4$

- Copper stabilizer plates for kink mode stabilization

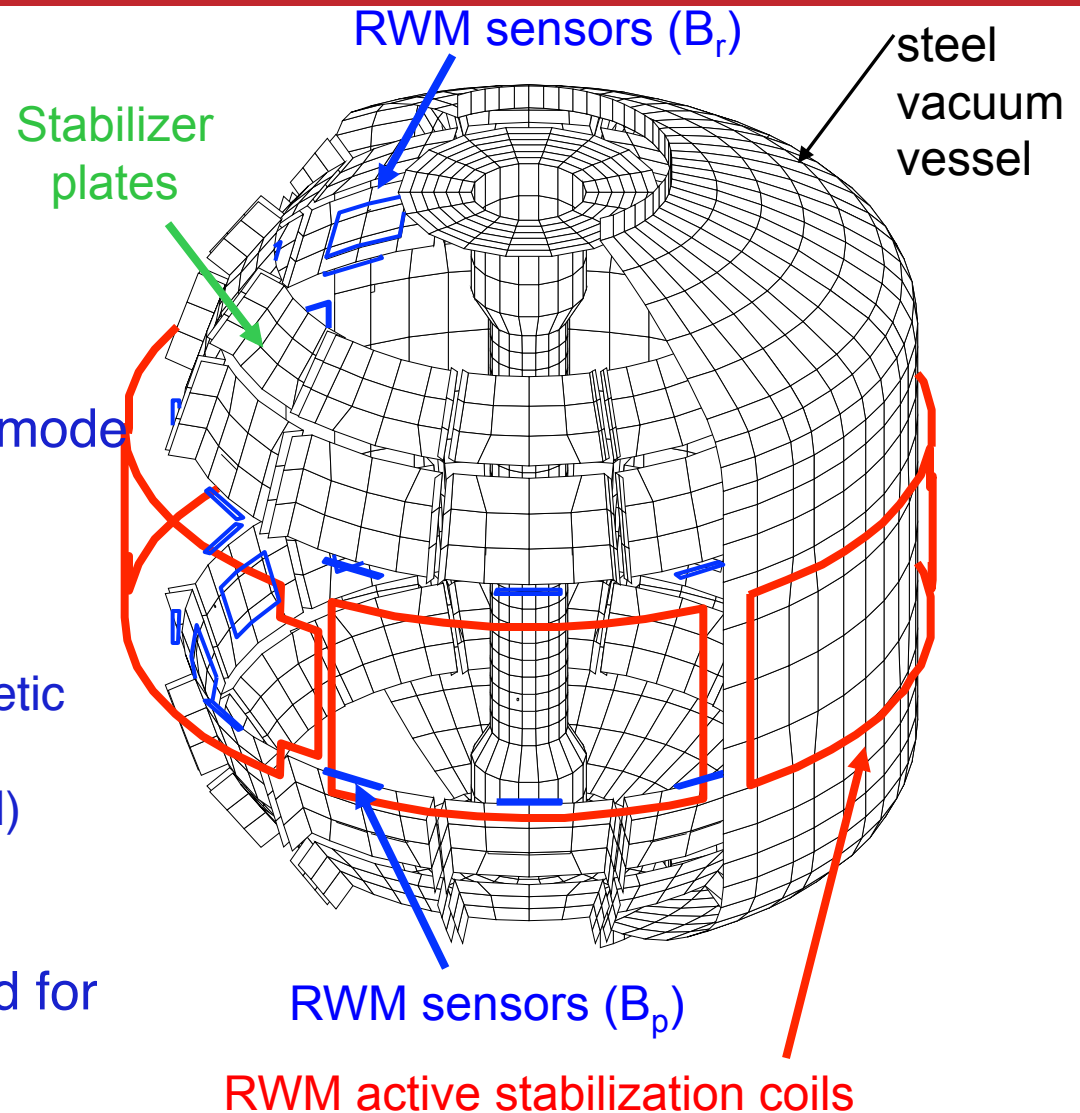
- Midplane control coils

 - $n = 1 - 3$ field correction, magnetic braking of ω_ϕ

 - $n = 1$ resistive wall mode (RWM) control

- Varied sensor combinations used for RWM feedback

 - 48 upper/lower B_p , B_r



The multi mode VALEN formulation includes many ideal plasma eigenfunctions in addition to the 3-D wall and coils

- VALEN formulation of the Resistive Wall Mode uses R-L circuit equations. The plasma response to an external perturbation is

$$\Phi_{plasma}^{total}(\phi, \theta) = [P] \Phi_{plasma}^{external}(\phi, \theta)$$

- [P] is the 'plasma permeability' [dimensionless], and Φ is the magnetic flux [V*s] on the unperturbed surface of the plasma
- In single mode VALEN [P] depends on only the unstable plasma mode
- In multi-mode VALEN [P] depends on multiple modes (unstable & stable)
- The conducting walls, control coils, and magnetic sensors are represented by L-R circuit equations.

i.e., $[L]\{\dot{I}(t)\} + [R]\{I(t)\} = \{V(t)\}$

and $\{\Phi^{sensors}(t)\} = [M]\{I(t)\}$

VALEN equations, multi-mode & original formulation

FLUX on wall, coils, and unperturbed plasma surface from

$$\{I_w(t)\} = \text{wall currents}, \quad \{I_c(t)\} = \text{coil currents},$$

$$\{I_d(t)\} = \text{dissipative plasma circuit currents}, \quad \{I_p(t)\} = \text{plasma mode currents}:$$

$$[L_{ww}]\{I_w(t)\} + [L_{wc}]\{I_c(t)\} + [L_{wp}]\{I_d(t)\} + [L_{wp}]\{I_p(t)\} = \Phi_w(t) = \Phi_{WALL}(t)$$

$$[L_{cw}]\{I_w(t)\} + [L_{cc}]\{I_c(t)\} + [L_{cp}]\{I_d(t)\} + [L_{cp}]\{I_p(t)\} = \Phi_c(t) = \Phi_{COIL}(t)$$

$$[L_{pw}]\{I_w(t)\} + [L_{pc}]\{I_c(t)\} + [L_{pp}]\{I_d(t)\} + [L_{pp}]\{I_p(t)\} = \Phi_p^{total}(t) = \Phi_{PLASMA}^{total}(t)$$

$$[L_{pw}]\{I_w(t)\} + [L_{pc}]\{I_c(t)\} + [L_{pp}]\{I_d(t)\} = \Phi_p^{external}(t) = \Phi_{PLASMA}^{external}(t)$$

$$\Phi_p^{external}(t) + [L_{pp}]\{I_p(t)\} = \Phi_p^{total}(t) = [P]\Phi_p^{external}(t)$$

where: plasma permeability $[P] = [\Lambda][L_{pp}]^{-1}$ and $[\Lambda]^{-1} = 2[G][\epsilon][G]^t$

$[G]$ = gram schmidt transformation and $[\epsilon]$ = ideal δW values (from DCON)

$$\text{i.e., } \{f_i(\theta, \phi)\} = A \sum_{\alpha} [G_{i\alpha}] \{b_{\alpha}^{DCON-Bn}(\theta, \phi)\}, \text{ and, } \oint \frac{f_i(\theta, \phi) f_j(\theta, \phi)}{A} da = \delta_{ij}, \oint da = A$$

VALEN equations, multi-mode & original formulation

single mode VALEN

$$[P] = \begin{pmatrix} -1 \\ s \end{pmatrix} \text{ or } [P] = \frac{\begin{bmatrix} -s & \alpha \\ -\alpha & -s \end{bmatrix}}{(s^2 + \alpha^2)} \text{ (with rotation)}$$

this is same as: $[P] = [\Lambda][L_{pp}]^{-1}$

$$s = -\Lambda^{-1}L = -2G_{11}\epsilon G_{11}L$$

$$G_{11} = \frac{1}{A \left[\oint B^n B^n dA / A \right]^{1/2}}$$

$$s = -\frac{2}{A^2} \frac{1}{\left[\oint B^n B^n dA / A \right]^{1/2}} \epsilon \frac{1}{\left[\oint B^n B^n dA / A \right]^{1/2}} L$$

$$s = \frac{-2L(\delta W)}{\Phi^2} = \frac{-\delta W}{LI^2/2}$$

multi-mode VALEN

$$[P] = [\Lambda][L_{pp}]^{-1} \text{ and } [\Lambda]^{-1} = 2[G][\epsilon][G]'$$

$$[\epsilon] = \begin{bmatrix} \delta W_1 & 0 & 0 & 0 & 0 & \dots \\ 0 & \delta W_1 & 0 & 0 & 0 & \dots \\ & & \delta W_2 & 0 & 0 & \dots \\ & & 0 & \delta W_2 & 0 & \dots \\ \cdot & & & & & \\ \cdot & & & & & \\ 0 & 0 & 0 & 0 & \dots & 0 & \delta W_n & 0 \\ 0 & 0 & 0 & 0 & \dots & 0 & 0 & \delta W_n \end{bmatrix}$$

or (with rotation)

$$[\epsilon] = \begin{bmatrix} \delta W_1 & \Gamma_1 & 0 & 0 & 0 & \dots \\ -\Gamma_1 & \delta W_1 & 0 & 0 & 0 & \dots \\ & & \delta W_2 & \Gamma_2 & 0 & \dots \\ & & -\Gamma_2 & \delta W_2 & 0 & \dots \\ \cdot & & & & & \\ \cdot & & & & & \\ 0 & 0 & 0 & 0 & \dots & 0 & \delta W_n & \Gamma_n \\ 0 & 0 & 0 & 0 & \dots & 0 & -\Gamma_n & \delta W_n \end{bmatrix}$$

VALEN equations (continued), & post processing to obtain B_{normal} from DCON modes on the plasma surface

single mode VALEN

solve for surface current potential:

$$g(\vec{r}) \quad \text{or} \quad g(\theta, \phi)$$

$$\vec{J} = \nabla \times g \hat{n} \delta(\vec{r} - \vec{r}_{surface}) \quad \text{and}$$

$$\vec{B}_{normal}^{DCON}(\vec{r}) = \frac{\mu_0}{4\pi} \nabla \times \oint_{\text{plasma surface}} \frac{\vec{J}(\vec{r}')}{|\vec{r} - \vec{r}'|}$$

calculate one plasma L using $g(\vec{r})$

multi-mode VALEN

use gram schmidt vectors $\{f_i\}$ for plasma surface current potential

$$\vec{J}_i(\vec{r}) = \nabla \times f_i(\vec{r}) \hat{n}_{surface} \delta(\vec{r} - \vec{r}_{surface})$$

calculate all plasma L_{ik} using $f_i(\vec{r})$ & $f_j(\vec{r})$

multi-mode post processing

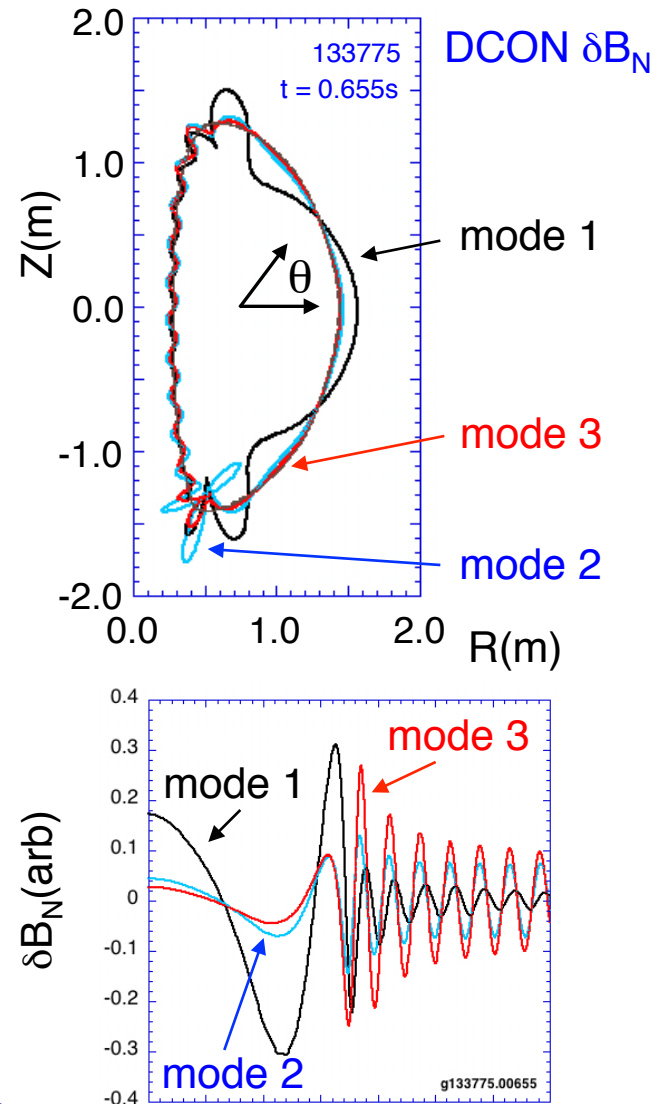
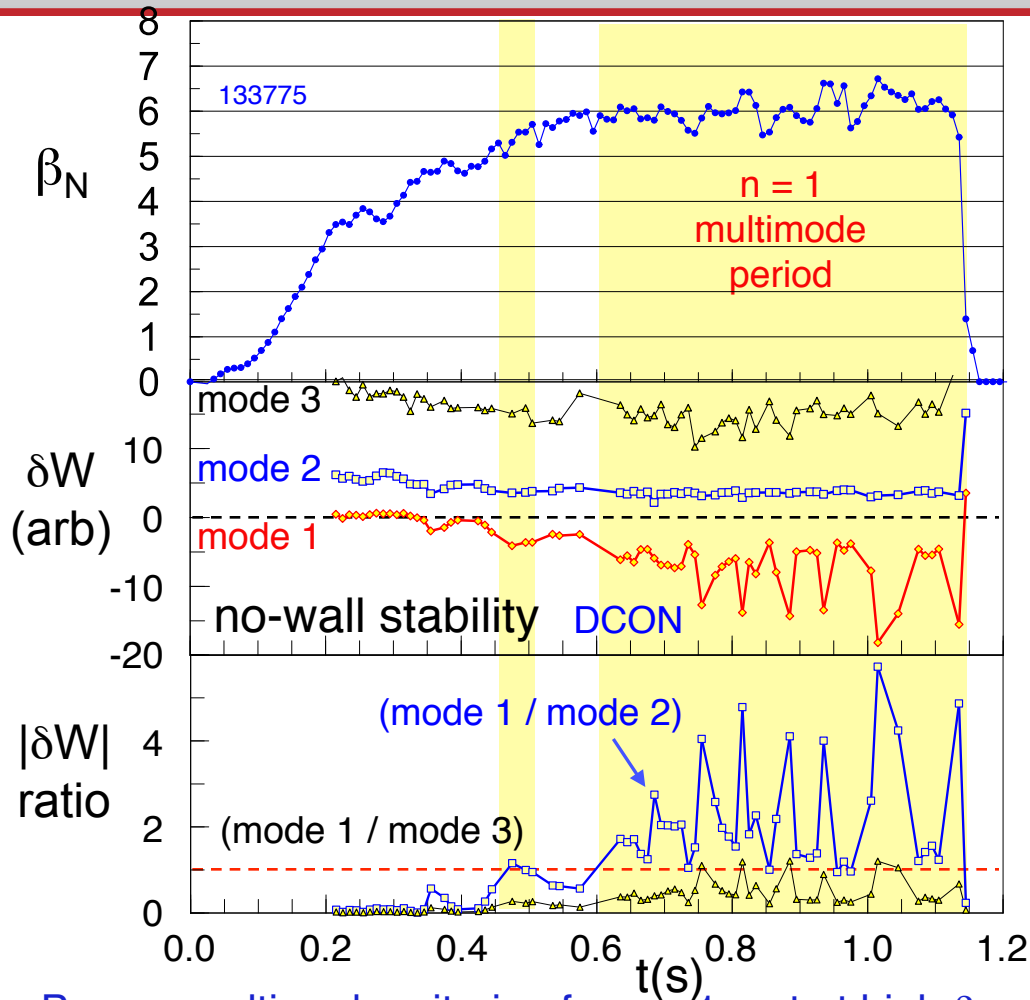
$$\{I_p\} = \left[L_{pp}^{mod es} \right]^{-1} ([P] - [1]) \left\{ \left[L_{pw}^{plasma-wall} \right] \{I_w\} + \left[L_{pc}^{plasma-coil} \right] \{I_c\} + \left[L_{pp}^{plasma} \right] \{I_d\} \right\}$$

B_n (gram schmidt functions) $\longrightarrow \left\{ \vec{B}_{plasma}(t) \cdot \hat{n}_{surface}(\theta, \phi) \right\}_i = \left\{ \left[L_{pp} \right]_{ij} \left(\left(f_j(\theta, \phi) \right) I_j^{plasma}(t) + \left(f_j(\theta, \phi) \right) I_j^{plasma} \right) \right\} / A$

recall: $f_j(\theta, \phi) = [G]_{jk} B_{DCON_mode}^n(\theta, \phi)$

B_n (DCON eigenmodes) $\longrightarrow \left\{ B^{normal}(\theta, \phi, t) \right\} = \left\{ \left[L_{pp} \right]_{ij} \left(\left([G]_{jk} B_{DCON_mode}^n(\theta, \phi) \right) I_j^{plasma}(t) + \left([G]_{jk} B_{DCON_mode}^n(\theta, \phi) \right) I_j^{plasma} \right) \right\} / A$

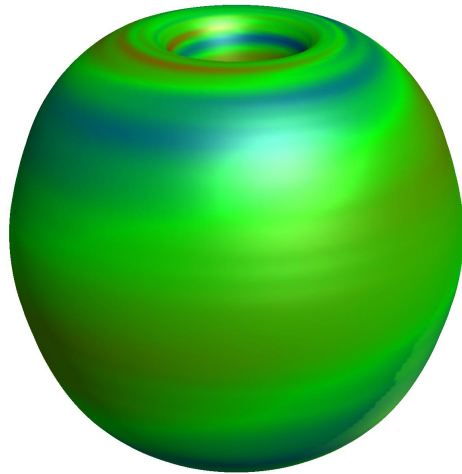
Multimode response theoretically is expected to be significant at high β_N



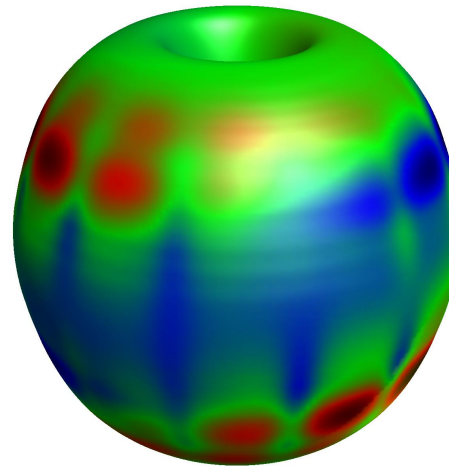
- Boozer multimode criterion for $n = 1$ met at high β_N
 - $|\delta W|$ smallest for 2nd $n = 1$ eigenfunction (PoP 10 (2003) 1458.)
 - Ratio of $|\delta W|$ for 3rd vs. 1st least stable mode sometimes also > 1

Passive growth @ $\beta_N = 5.54$ multi mode VALEN results for NSTX shot 133775.00495

total B_n on plasma surface



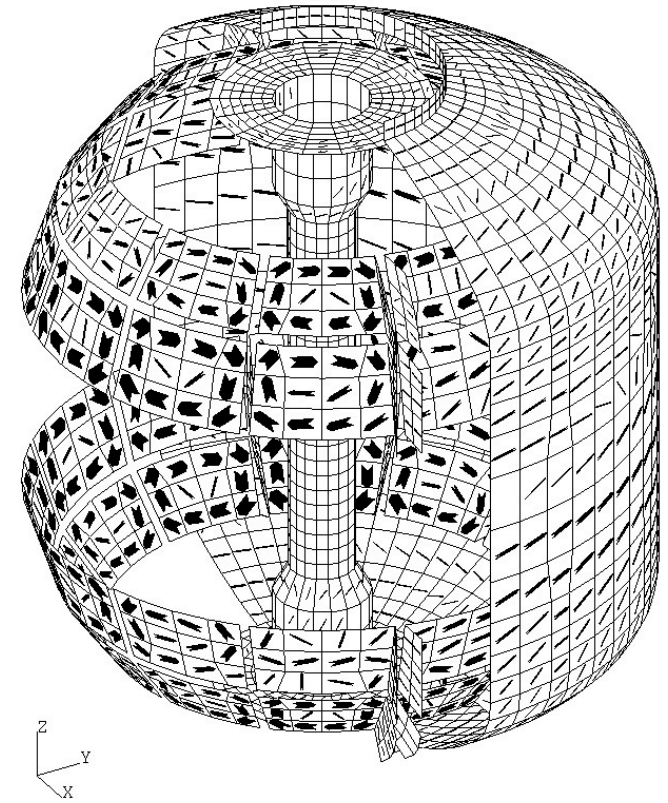
B_n on plasma surface from only wall currents



cut away view of wall currents

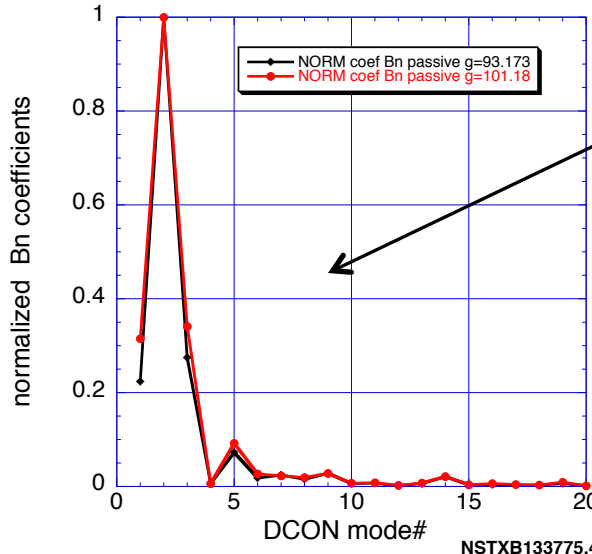
$\beta_N = 5.54$

growth rates = 93, 101 [1/s]



color contours: dark red ~big negative, green ~ zero, dark blue ~ big positive

Multi-mode spectra passive RWM in NSTX @ $\beta_N=5.54$



relative weight of DCON modes in passive growing RWM

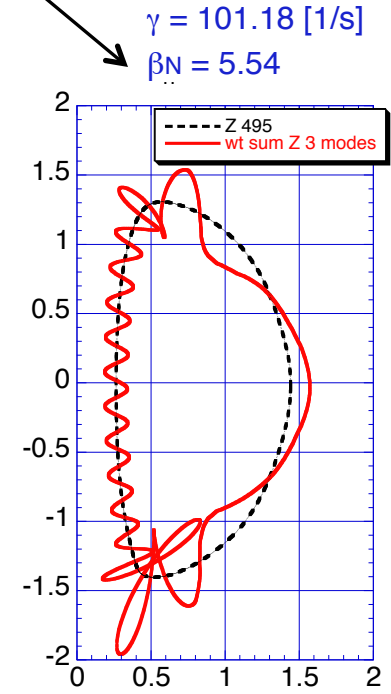
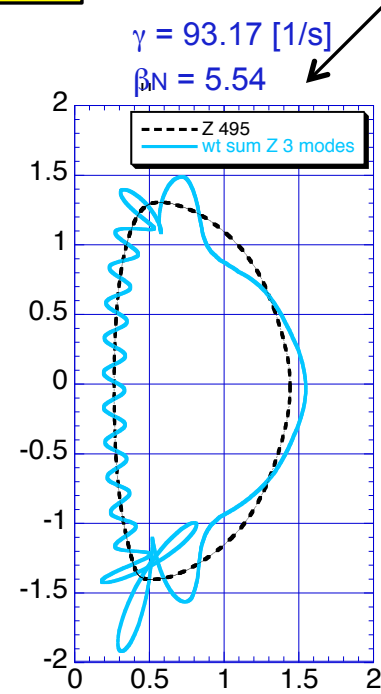
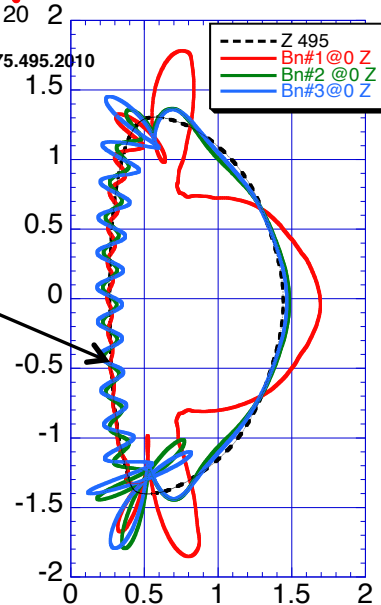
NSTX shot #133775
t = 0.495 [s]

DCON mode weighted sums shown below
Illustration of B_normal signature for RWM mode
normal distance from plasma surface corresponds to B_normal

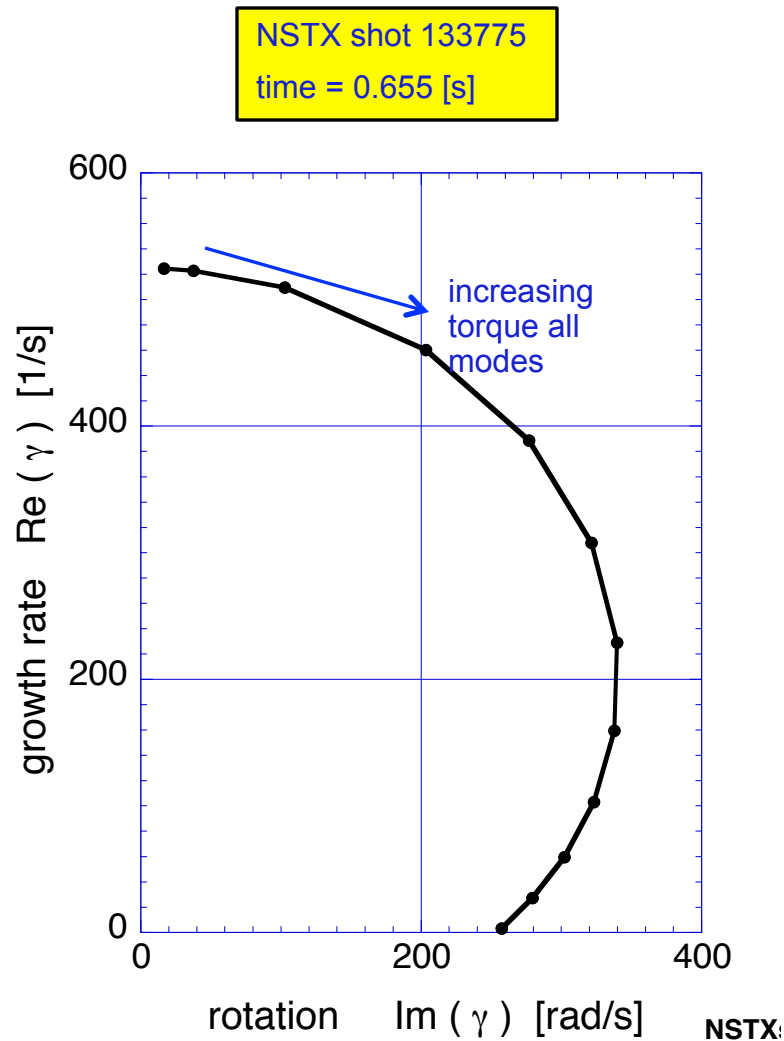
Illustration of DCON modes equal weights

#1 thru #3,
each DCON mode shown with max B_n = 0.5[m]

normal distance from plasma surface (black dashed line) corresponds to B_normal



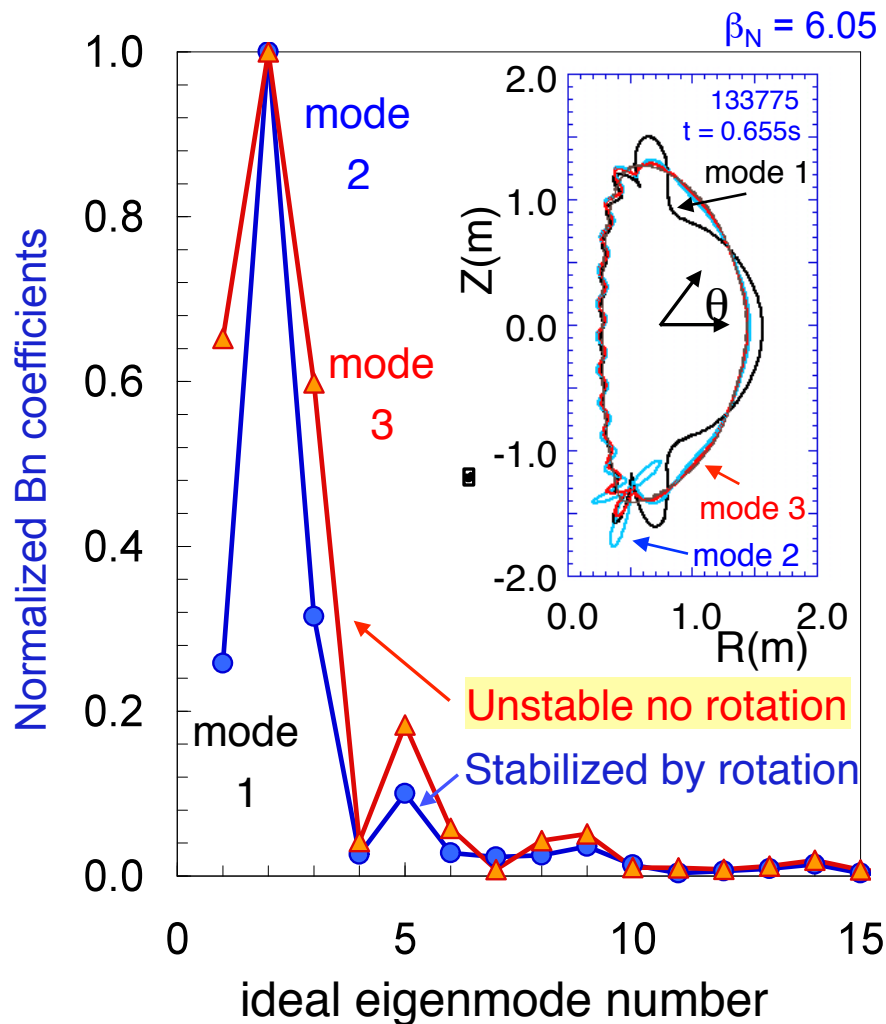
Mode may be stabilized by rotation alone, VALEN predicts RWM growth rate as same torque is applied to all modes



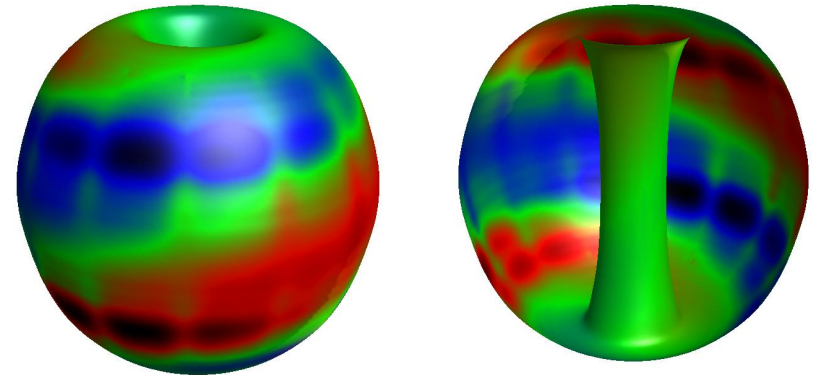
- NSTX RWM stabilized by ω_ϕ
- VALEN calculation of rotation needed for stabilization ~ 41 [Hz] is close to experimental value of ~ 30 [Hz]
- $\beta_N = 6.05$

VALEN multi-mode RWM computation shows 2nd eigenmode component usually has dominant amplitude in NSTX at high β_N

δB^n RWM multi-mode composition



δB^n from wall, multi-mode response



- NSTX unstable RWM
 - Computed growth time consistent with experiment
 - 2nd eigenmode (“divertor”) has larger amplitude than ballooning eigenmode
- NSTX RWM stabilized by ω_ϕ
 - Ballooning eigenmode amplitude decreases relative to “divertor” mode

RWM feedback control: Mathematics of VALEN feedback for NSTX

- Analyze upper Bp sensor signals in NSTX for selected 'n' to identify RWM
- Compensate for control coil flux in sensors
- Scan phase angle between the RWM signal and the pattern of voltage applied to the control coils
- Choose gain for feedback [v/flux]
- Run multi-mode VALEN eigenvalue calculation and predict growth rate
- Feedback may cause the plasma modes to rotate

use classic least squares fitting to find S & C :

$$S * \sin(n * \phi_1^{sensor}) + C * \cos(n * \phi_1^{sensor}) = \Phi_1^{sensor}$$

$$S * \sin(n * \phi_2^{sensor}) + C * \cos(n * \phi_2^{sensor}) = \Phi_2^{sensor}$$

⋮

$$S * \sin(n * \phi_N^{sensor}) + C * \cos(n * \phi_N^{sensor}) = \Phi_N^{sensor}$$

$$\text{or } [A]_{Nx2} \begin{Bmatrix} S \\ C \end{Bmatrix}_{2x1} = \{\Phi^{sensor}\}_{Nx1}$$

where : sensors located at angles ϕ_i

and sensors read magnetic flux Φ_i

solution is :

$$\begin{Bmatrix} S \\ C \end{Bmatrix} = ([A]^T [A])_{2x2}^{-1} [A]_{2xN} \{\Phi^{sensor}\}_{Nx1}$$

voltages applied to coil are :

$$\begin{Bmatrix} V_1^{coil} \\ \vdots \\ V_C^{coil} \end{Bmatrix} = G_p \begin{bmatrix} \sin(\phi_1^{coil} + \delta) & \cos(\phi_1^{coil} + \delta) \\ \vdots & \vdots \\ \sin(\phi_C^{coil} + \delta) & \cos(\phi_C^{coil} + \delta) \end{bmatrix} ([A]^T [A])_{2x2}^{-1} [A]_{2xN} \{\Phi^{sensor}\}_{Nx1}$$

where : coils located at angles ϕ_i^{coil}

and we use phase δ

to provide compensation for coil to sensor coupling

$$\text{replace } \{\Phi^{sensor}\}_{Nx1} \text{ by } \{\Phi^{sensor}\}_{Nx1} - [M_{sensor,coil}]_{NxN} \{I^{coil}\}_{Cx1}$$

RWM feedback control: VALEN results, scan in feedback phase for $\beta_N = 4.65$

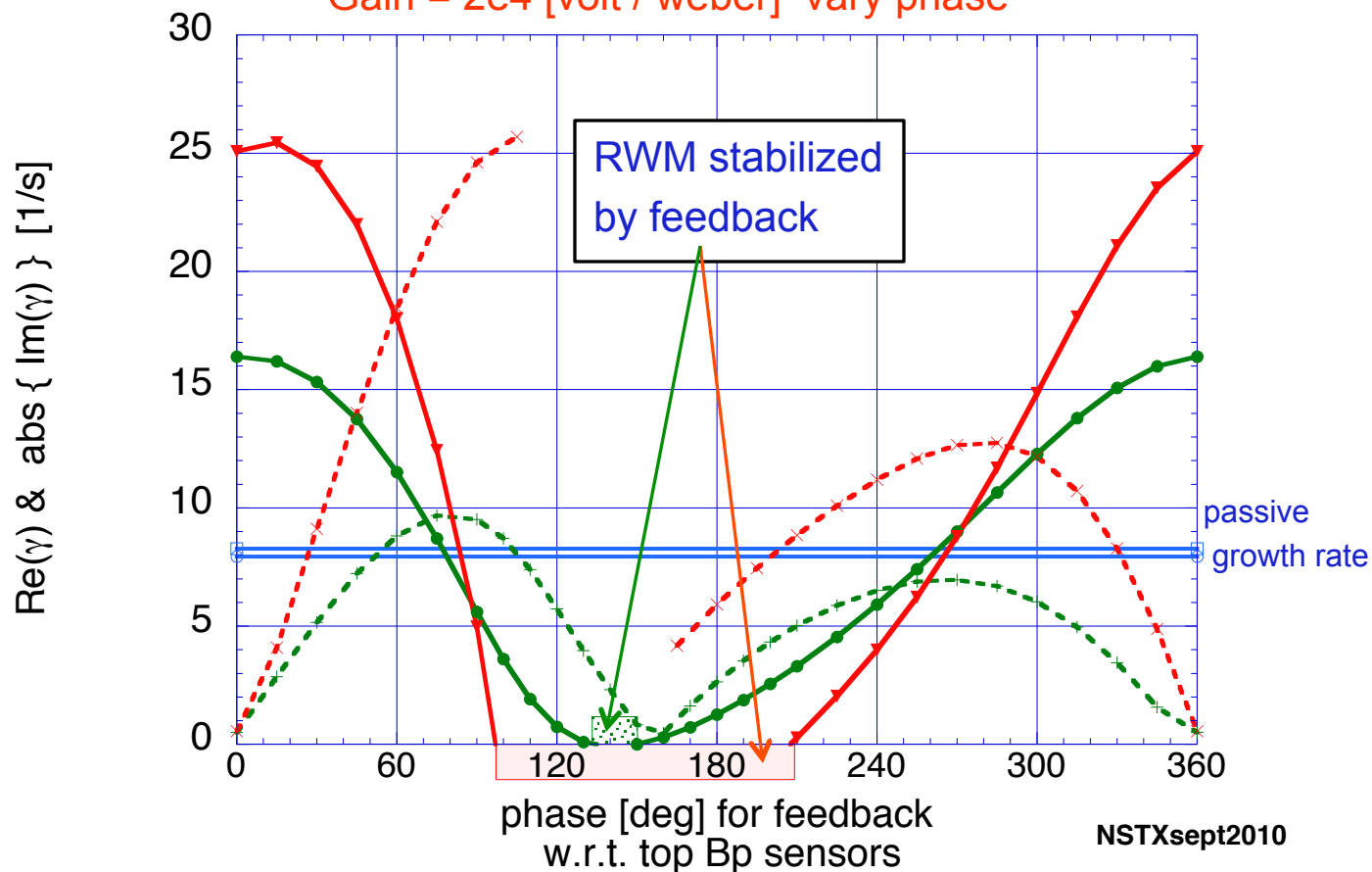
NSTX shot #133775
t = 0.345 [s]

VALEN eigenvalue calculations with feedback

Gain = 1e4 [volt / weber] vary phase

Gain = 2e4 [volt / weber] vary phase

- Notes:
- solid lines show growth rate
- dashed lines show rotation
- shaded regions indicate RWM is stabilized by feedback
- horizontal lines show passive growth rate without feedback



RWM feedback control: VALEN results, scan in feedback phase for $\beta_N = 5.54$

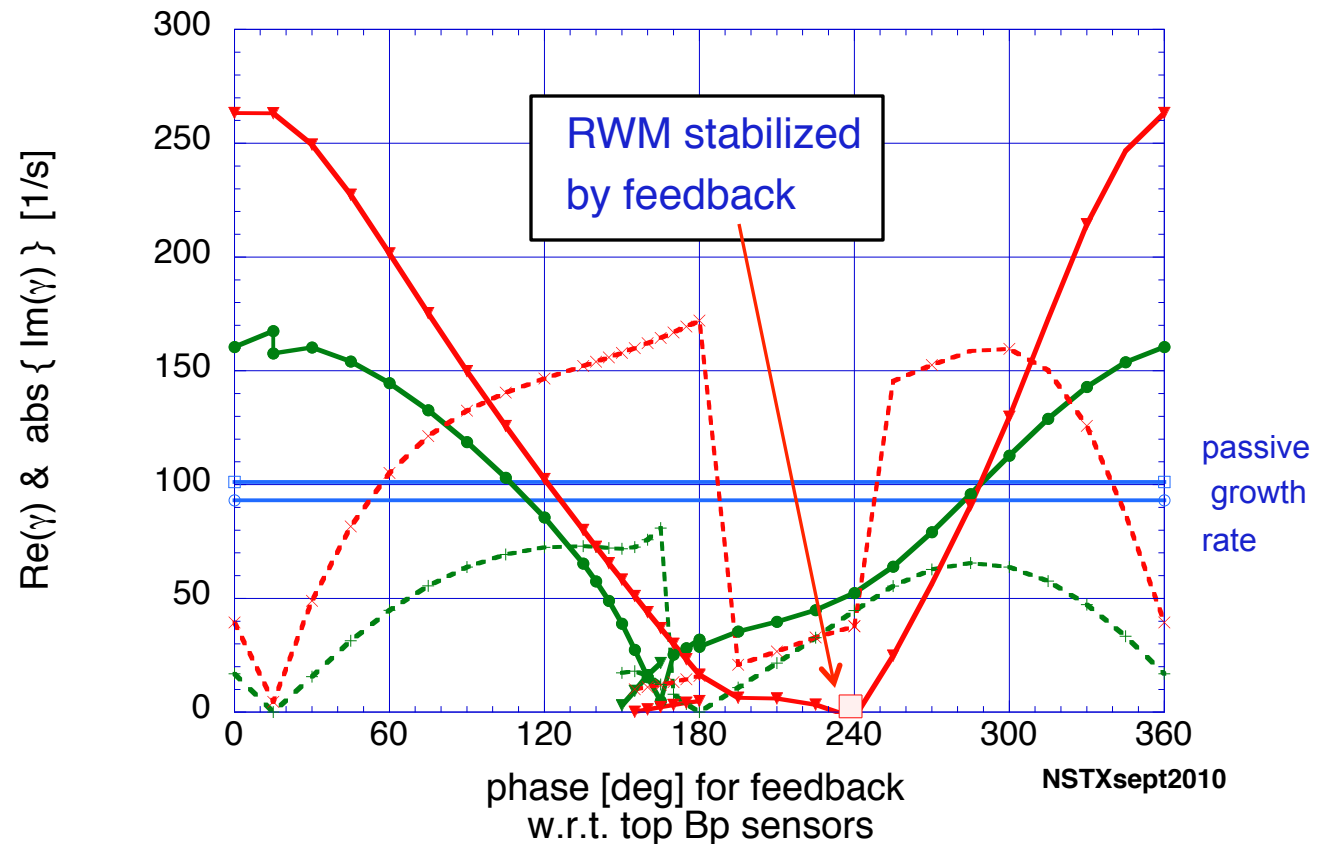
- Notes:
- solid lines show growth rate
- dashed lines show rotation
- horizontal lines show passive growth rate without feedback
- only a small region at $G=1e5$ near phase = 240 is stabilized when $\beta_n=6.079$

NSTX shot #133775
t = 0.495 [s]

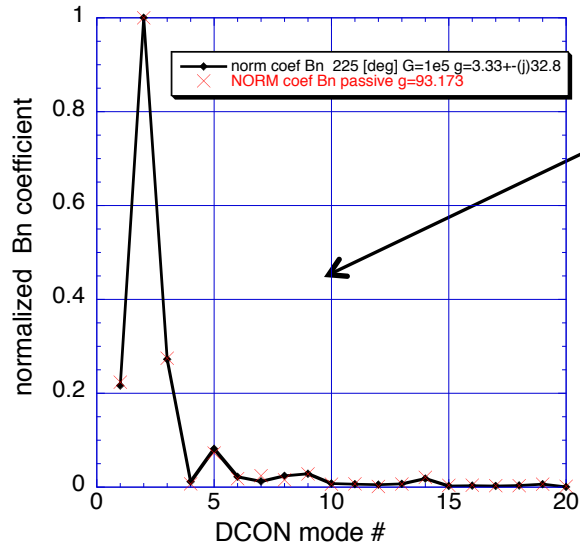
VALEN eigenvalue calculations with feedback

Gain = $4e4$ [volt / weber] vary phase

Gain = $1e5$ [volt / weber] vary phase



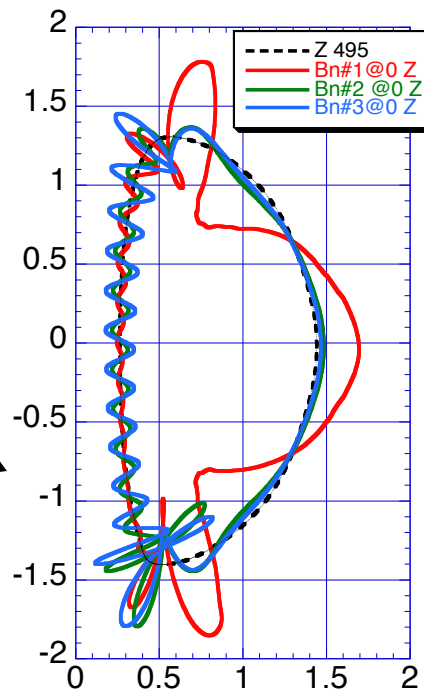
Multi-mode spectra with RWM feedback in NSTX @ $\beta_N = 5.54$



- relative weight of DCON modes in RWM with feedback $G=1e5$, phase=225 [deg]
- x relative weight of DCON modes for passive RWM growth

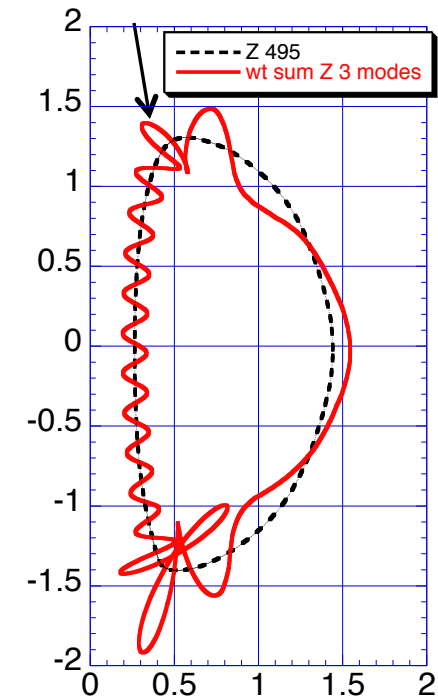
NSTXB133775.495.2010

Illustration of DCON modes #1 thru #3, each DCON mode shown with max $B_n = 0.5$ [m] (equal weights) normal distance from plasma surface (dashed black line) corresponds to B_{normal}



DCON mode weighted sums shown below

Illustration of B_{normal} signature for RWM mode with feedback
normal distance from plasma surface corresponds to B_{normal}



Summary - Conclusions

- ❑ Control of RWM is important, allows sustained access to high beta regimes
- ❑ Multi mode VALEN predictions, both passive growth and performance with applied feedback consistent with experimental observations in NSTX
- ❑ Multi mode VALEN calculations indicate lowest order modes dominate the RWM response, both passive and with active feedback
 - ❑ The second (stable) DCON mode has the greatest contribution for simple passive growth, passive growth with substantial mode rotation, and when feedback is applied
- ❑ Future work planned includes further application to NSTX experimental results, studies of error field amplification, and application of RWM feedback logic both in the time domain and frequency domain.